On prediction of the compressive strength and failure patterns of human vertebrae using a quasi-brittle continuum damage finite element model

Zahira Nakhli, Fafa Ben Hatira, Martine Pithioux, Patrick Chabrand, Khemais Saanouni

▶ **To cite this version:**

Zahira Nakhli, Fafa Ben Hatira, Martine Pithioux, Patrick Chabrand, Khemais Saanouni. On prediction of the compressive strength and failure patterns of human vertebrae using a quasi-brittle continuum damage finite element model. Acta of Bioengineering and Biomechanics, 2019, 21 (2), pp.143-151. ⟨10.5277/ABB-01265-2019-03⟩. ⟨hal-02114927⟩

HAL Id: hal-02114927

https://hal.science/hal-02114927v1

Submitted on 30 Apr 2019

HAL is a multi-disciplinary open access archive for the deposit and dissemination of scientific research documents, whether they are published or not. The documents may come from teaching and research institutions in France or abroad, or from public or private research centers.

L'archive ouverte pluridisciplinaire **HAL**, est destinée au dépôt et à la diffusion de documents scientifiques de niveau recherche, publiés ou non, émanant des établissements d'enseignement et de recherche français ou étrangers, des laboratoires publics ou privés.

Distributed under a Creative Commons CC BY-NC 4.0 - Attribution - Non-commercial use - International License

A Quasi-brittle Fracture FE model for vertebrae bone with an experimental validation

Fafa ben Hatira[1], Zahira Nakhli[2], Martine Pithioux[3], Patrick Chabrand[4], Khemais Saanouni[5]

1; 2 Laboratoire de Recherche : Matériaux, Mesures et Applications
Département Génie Physique et Instrumentation
INSAT, BP 676 1080 Tunis Cedex

3 :4 Aix Marseille Univ, CNRS, ISM, Inst Movement Sci, Marseille, France

[5] ICD/LASMIS, UMR STMR 6279, Université de Technologie de Troyes, 12 rue Marie Curie-BP2060, 10010 Troyes, France

A Quasi-brittle Fracture FE model for vertebrae bone with an experimental validation

The purpose of this study is to present a numerical treatment of a quasi-brittle damage constitutive model to help surgeons while making decision for patient suffering from fractures. Most of the presented material models, found in the literature which deals with damage, are complex and they depend on a large number of parameters. Therefore, the simplicity of the model introduced in this work to describe the damage of vertebra (healthy or pathologic) reveals its real efficiency to predict the crack localization for different types of vertebrae.

A quantitative computed tomography (QCT)-based finite element method (FEM) model is developed within the framework of continuum damage mechanics (CDM). It describes both the initiation and the progressive propagation of cracks which will help predicting the fracture of a human vertebrae by reproducing the experimental failure of four cadaveric lumbar vertebral bodies (female=1, male=3, age = 82 ± 9 years) under quasi-static compressive loading paths.

To achieve this goal, different steps have been taken to propose a new bone damage law. First, the six CT scanned vertebra experimental data obtained is presented. Then, a theoretical damage model is introduced. The damage initiation prediction results and crack progressive propagations are presented. Finally, the proposed models with different elastic modulus estimation comparison show a good agreement between the numerical and the experimentally measured force- displacement curves as well as the damage localization. The numerical models are implemented into the finite element code (ABAQUS).

Keywords: Vertebrae fracture, damage law, elastic modulus, finite element analysis

Subject classification codes: include these here if the journal requires them

Introduction

The motivation of this research is to provide valuable improvement for the surgical diagnosis and aims at reducing healthy and osteoporotic vertebrae fractures, as well. The originality of this paper is the quasi-brittle law simplicity describing the bone damage in such cases like cars' crash or severe fall.

In this study, numerical models are developed and implemented in order to identify vertebral fracture over expected experimentally compression load ranges. Thanks to this study, answers are given to questions about the damage affecting vertebral bodies, such as the ultimate load magnitude as well as the damage state of all vertebrae.

The osteoporosis that is affecting more and more people (man and woman) is a disease which characterized by the bones 'weakness that increases the risk of their breaking. It is an age-related disease which causes progressive skeletal disorder characterized by a low bone mass and microarchitectural alterations increasing bone fragility and susceptibility to fracture [1].This causes pain and a significant loss of mobility. Vertebral fractures are the most [2] common type of osteoporotic fracture and they are associated to the decreasing quality of life [3] and to the substantial morbidity [4].

Clinically speaking, osteoporosis is diagnosed using the dual-energy X-Ray absorptiometry (DXA) [2, 5, 6]. The system measures the bone mineral density (BMD). The fracture risk is assumed to be highly correlated with the value measured by the DXA. Osteoporosis is defined for bones with a BMD between 833 and 648 mg/cm^2 (equivalent to a T-score between -1.0 and -2.5), whereas if a BMD is above 833 mg/cm^2 (T-score above -1.0), they are considered as healthy. Experts give osteoporosis medications with a BMD less than 648 mg/cm^2 (T-score less than −2.5). It is also noteworthy that DXA is submitted to restrictions for the assessment of bone fragility and osteoporosis diagnosis [7]. DXA is based on 2D and not 3D measurements and used only for porous bone information and not for compact bone. It is known that microarchitecture alteration is currently included in the definition of osteoporosis [1].
From a numerical point of view, several FE model describing damage and fractures for bone structure are proposed in the literature. Most of these works introduce linear and non-linear isotropic and anisotropic finite element (FE) models. Each work presents a new model with some answers about the best way to predict bone structures damage. Doblaré et al [8] present a study of the proximal femoral extremity remodeling based on an anisotropic bone model and state that the evolution of bone microstructure internal variables can be formulated following the Continuum Damage Mechanics (CDM) principles.

They show that a good similarity is obtained between numerical and experimental results**.** The same authors present [9] another work for both hard and soft tissues. A damage-bone remodeling theory presented in [10] shows that under constant load, the three unit bone bars structure exhibit inhomogeneous strains which strongly depend upon the manner in which the microdamage is distributed

To emphasize the distinct damage behavior in tension and compression, Garcia & al presented in [11] 3D anisotropic constitutive equations. For the sake of simplicity, Hambli et al ([12], [13]) presented in these two works respectively a simple finite element (FE) model coupled with quasi-brittle damage model for the proximal femoral fracture prediction based on orthotropic behavior and a numerical FE-based model with an element deletion to describe the cracks propagation. Many Quantitative computed tomography (QCT)-based finite element (FE) voxel models have been presented to predict ultimate force of human lumbar vertebrae under axial compression. As mentioned in [14], no clear choice of the failure criterion to adopt for the bone tissue has been found to predict fracture risk of bones. In that work, a combined experimental-numerical approach has been used to build up a subject-specific finite element models which are able to accurately predict failure patterns of bones. In [15] a theoretical model formulated within the framework of continuum damage mechanics and based on fabric tensor is proposed. A good correlation between experimental and numerical results has been found. The authors of [16] proposed an original bone remodeling law coupled to trabecular bone plasticity for the simulation of orthodontic tooth movements by using a phenomenological approach of anisotropic Continuum Damage Mechanics. Over the last decades, developments in (3D) have provided possibilities for measuring a variety of structural indices to characterize bone microarchitecture. However, standard mechanical tests did not provide easily the elastic constants due to the small size of specimens of human bone. The dependency of microarchitecture on bone's mechanical properties has been presented in [17, 18]. The authors showed that the elastic constants, specifically the young's modules are clearly correlated with the tissue morphology bone coefficient BV/TV. The results presented in [19] indicate that there is no universal modulus–density relationship for on-axis loading. The authors suggest that the site-specificity in apparent modulus–density relationships may be attributed to the

differences in architecture. In [15], authors showed that there is a strong correlation between cumulated permanent strain and elastic modulus which indicate that these variables affect the damage process. For isotropic cellular materials, a basic model consists of a power relationship of the Lamé constants with respect to volume fraction [20]. For anisotropic materials, an averaging method was developed by Cowin et al in [21] to identify the type of elastic symmetry and express the dependency of the elastic constants toward the volume fraction in [22].

In general, most of the articles found in the literature show how it is important to provide a precise diagnosis of fracture state (magnitude and localization) and how to give different answers for different types of bone (healthy or not), and how to establish behavior model to quantify the bone fracture. However, they showed controversies in different conclusions on the same topic.

As it has been reported in [12, 13] a quasi-brittle damage model coupled to an orthotropic behavior law can predict the proximal femur fracture. In [46], the authors present a study to predict the failure of human vertebra based only the strength level and failure patterns.

Our model based on a simple isotropic damage law gives a unified and reliable answer to different quality of bones and precisely predict the ultimate fracture load as well as the damage localization for vertebra.

Studies found in the literature followed different approaches to estimate the Young modulus. For example, authors of [15, 33] reported that the mechanical behavior of trabecular bone is mainly governed by its tissue modulus and morphology, i.e. bone volume fraction (BV/TV) especially in the case of small strain. In studies [47, 48, 49, 50] , authors adopted elasticity– apparent density relationships to build FE models.

In the present work, three simple methods proposed in different works in the literature computing the Young's modulus E (MPa) that have been implemented in the numerical model in order to compare them and to show their performance toward reproducing the initiation and the propagation of the damage. The first method is based on the" grey value ". The second method has been proposed by Yang et al in [22]. Finally, the third one is presented by Hernandez in [23]. These three methods are going to be presented in the next section.

- Method 1: Many researchers such as Jacobs et al [24], Keyaketal [25], Helgason et al [26], Madi et al. [27], Tawara et al [28], and Jovanovici et al [29], Gislanson et al [30] showed that the Young's modulus for each finite element depends on the apparent density for each bone voxel ($E = f(\rho)$), which in its turn was calculated on the basis of CT images. Relationship between the apparent density and CT values (HU: Hounsfield Units or GV: gray values) is also calibrated. The chosen formula can be expressed as:

$$E = 3500\,\rho^{2.2} \qquad (1)$$

- Method2: In [22], Yang et al propose a dependent orthotropic Hooke's model for cancellous bone based on the identification of the elastic constants of trabecular bone in function of volume fraction (BV/TV).

$$E = 1240 E_T \left(\frac{BV}{TV}\right)^{1.8} \qquad (2)$$

Where E_T is the slope obtained from the experimental curves (see Figure.3)

- Method 3: In [23], Hernandez et al present the used parameters to predict bone material properties with power law functions of the form:

$$y = ax^{b} \quad (3)$$

Where y is the strength or elastic modulus, x a parameter (i.e apparent density) and a and b are empirical constants derived from experimental data. They propose the following relationship where the x on the preceding power function is the bone volume / total volume ratio (BV/TV):

$$E = 84370\left(\frac{BV}{TV}\right)^{2.58} \quad (4)$$

In what follows the material, the experimental method and the numerical models with the obtained results are going to be detailed. The first one introduces the procedure to obtain data and geometry of the six CT scanned lumbar vertebra, followed by the experimental curves obtained for the vertebrae tested under compression till fracture. As pointed out previously, Continuum Damage Mechanics 'CDM' framework is chosen since it is the most appropriate constitutive framework to reproduce the bone structure failure as it will be detailed in section 2.In the third part, the boundary and load conditions are presented. The simulations of different cases are detailed in section 4 for the sake of a comparison between theoretical and experimental results.

1. Material and Method

1.1 Sample preparation

Six lumbar vertebrae obtained from four donors (female=1, male=3, age = 82 ± 9 years [range: 63 – 91]) were CT scanned by using a GE Medical Systems scanner available in La Timone University hospital, (Marseille. DICOM images files generated by the scanner are constituted by pixels with different gray intensities). The investigations were approved by research ethics board at the University Hospital.

- Step 1: 3D reconstruction has been accomplished using the technique of density segmenting with the research software Mimics 17.0. The generation of the surface and volume meshes was made by the research software 3Matic 9.0.0.231. It was used to create a triangular mesh on the surface of the vertebra, and to generate the volume mesh with linear tetrahedral elements (C3D4, six degrees of freedom per node). The volume mesh was imported again in Mimics, in order to assign the material parameters based on the Hounsfield Units 'HU' or Units Gray values on the scanned images. The density ρ and the young Modulus E are obtained at the end of this step and the geometry is used in the finite element simulation.

- Step 2: Through the software Image J combined with the software Bone J, the architectural parameters were extracted: BV/TV (Bone Volume over Total

volume; i.e. bone volume fraction), Tb.Th (trabecular thickness), Tb.Sp (Trabecular Spacing) and Tb.N (Trabecular Number). These parameters were also used in the finite element computations.

In Figure 1, the flow chart summarizes the protocol established to create FE models from CT data using material properties is presented following the steps detailed previously.

1.2 Experimental Mechanical Compression test

One of the most used classifications of type of trauma is the one introduced by Magerl [31] based on the morphological analysis of lesion. The called type A is attributed to the compression injury. It is subdivided into three types (Group A1 fracture on the top of the vertebra; A2 Group fracture separation; A3 Group, burst-fracture [32]. To reproduce the trauma produced by cars' crash or severe fall, compression of lumbar vertebra investigations were performed on six lumbar vertebrae obtained from four human cadavers. An INSTRON 5566 device was used for the compression test. Vertebrae with embedded epoxy resin were placed between the jaws (Figure 2a). Resin was maintained during the entire test enabled vertebrae to be set in the vertical axis of the compression device. A velocity of 5 mm/min was imposed during the test. The failure load (in kN) and displacement were measured. During the mechanical test, the mean failure load was (2.4kN). The initial crack always occurred in the middle of the vertebra .Experimental ultimate load, final displacement, BMD for all vertebrae are reported in Table 1.

The next picture (Figure 2b) taken during the compression of one of the specimens, show clearly that the failure occurs in the middle of the vertebra with the wedge fracture which is close to the group A3 with a reduction of the height of the vertebra.

In Figure 3, the experimental data obtained for the six specimens are reported. The value of the tangent modulus E_T used in the second method for young's modulus estimation 2 (Eq.2) are mentioned in the same curves. The maximum value (E_T= 39 MPa) is obtained for the specimen 3-L2, whereas the lowest one (E_T= 7 MPa) is obtained for the specimen 2-L2. It seems clear that this value depends on the classification of vertebra (healthy or osteoporotic). Indeed, specimen 3, which is reported as healthy, has a BMD of 0.884, whereas, specimen 2, which is reported as osteoporotic, has a BMD of 0.616. The load-displacement curves obtained for three different vertebrae (L2, L3, L4) taken for the same donor (specimen 3), showed the same tendency with a variation in the fracture load magnitude [33].Indeed, taken in the same segment, the different lumbar vertebrae will not have the same orientation with respect to the vertical axis of the standing or sitting position. Therefore the same compression forces will act differently on them depending on the position of the vertebra in the spine segment.

In order to reproduce the obtained experimental data as the localization of the crack, the state of damage , the ultimate load failure, a new CDM model coupled with the three young modulus (equations1, 3, 4) is presented in the next section.

2. Bone constitutive models

2.1. Constitutive framework: A quasi brittle damage law

The approach of irreversible thermodynamics with internal variables (Chaboche [34], Germain [35], Krajcinovic [36], Saanouni [37], Lemaitre [38], Kachanov

[39]), is chosen to present a coupled damage elastic model to describe the initiation and the accumulation of the damage in bone structure, more precisely the vertebra.

In this work, the damage behavior law describing a quasi-brittle behavior is proposed using an isotropic Continuum Damage Mechanics (CDM) based on Marigo modeling of the damage for brittle and quasi-brittle material behavior [40]. This theory is formulated to describe the progressive degradation of material (CDM) models.

The new energy based model is described throughout state variable (external and internal).The state variables describing the constitutive equations are represented by the external and the observable variables, respectively the elastic strain tensor $\underline{\varepsilon^e}$and the Cauchy stress tensor $\underline{\sigma}$. For the sake of simplicity, damage is supposed isotropic described by a couple of scalar internal variables (D, *Y*) where *Y* is damage associated variable.

The effective variables $\underline{\varepsilon}^e$and $\underline{\sigma}$ including the damage effect which are defined in the framework of the elastic strain equivalence assumption are presented hereafter. The expression of the stored elastic energy density is given by:

$$\rho\psi\left(\underline{\varepsilon}^e, D\right) = \frac{1}{2}(1-D)\underline{\varepsilon}^e : \underline{\underline{A}} : \underline{\varepsilon}^e + \hat{\psi}(D) \quad (5)$$

Where $\underline{\underline{A}}$ is the symmetric fourth-rank tensor of elastic properties of the virgin (not affected by damage) material which in the isotropic case can be written in terms of the well-known Lame's constants λ and μ according to:

$$\underline{\underline{A}} = \lambda \underline{1} \otimes \underline{1} + 2\mu \underline{\underline{1}}$$

$$\mu = \frac{E}{(1-2\upsilon)};\ \lambda = \frac{E\upsilon}{(1+\upsilon)(1-2\upsilon)}$$

Where $\underline{1}$ is the second-rank identity (Kronecker) tensor while $\underline{\underline{1}}$ is a fourth-rank unit tensor.

According to the theory of Marigo, the free energy per unit mass $\hat{\psi}(D)$depends only on the two state variables namely the elastic strain tensor and the damage.

The state laws$\boldsymbol{\sigma}$ and Y are classically derived from the state potential are obtained from the free energy by:

$$\underline{\sigma} = \rho \frac{\partial \psi}{\partial \underline{\varepsilon}^e} = (1-D)\underline{\underline{A}} : \underline{\varepsilon}^e \quad (6.1)$$

$$\underline{\underline{A}} = \rho \frac{\partial^2 \psi}{\partial^2 \underline{\varepsilon}^e} \quad (6.2)$$

$$\underline{\sigma} = (1-D)\left(\lambda \underline{1} \otimes \underline{1} + 2\mu \underline{\underline{1}}\right) : \underline{\varepsilon}^e \quad (6.3)$$

$$Y = -\rho \frac{d\psi}{dD} = \frac{1}{2}\underline{\varepsilon}^e : \underline{\underline{A}} : \underline{\varepsilon}^e \quad (7)$$

The damage criterion (or damage yield function) is described by Y:

$$f(Y, D) = Y - \frac{1}{2}Y_0 - mD^{\frac{1}{s}} = 0 \quad (8)$$

Y_0, s and m are the material parameters.

The parameters s and m are related to the damage "hardening" of the material. It is here to be noticed that the damage yield function (8) can describe the initiation of micro-cracks starting from undamaged state (D=0).

In the present model, the dissipation potential $\boldsymbol{\varphi}$ is reduced to the yield function f (associative theory):

$$\varphi = f = Y - \frac{1}{2}Y_o - mD^{1/s} = 0 \quad (9)$$

The evolution laws derived from the dissipation potential are :

$$\dot{\varphi} = 0 \Leftrightarrow \frac{\partial \varphi}{\partial Y}\dot{Y} + \frac{\partial \varphi}{\partial D}\dot{D} = 0 \quad (10)$$

For this approach, the coupling between damage and elasticity is completed with the following damage evolution law.

$$\dot{D} = \frac{s}{m}\frac{\dot{Y}}{D^{\frac{1-s}{s}}} \quad (11)$$

With:

$$\dot{Y} = \underline{\varepsilon}^{e} : \underline{\underline{A}} : \dot{\underline{\varepsilon}} \quad (12)$$

The above presented model emphasizes on the fact that the damage evolution is the influent parameter since it will affect the young modulus degradation as well as the evolution of the Cauchy stress. It will implicitly produce the damage propagation.
Solving the nonlinear problem described by equations (6, 7,8,9,10,11 and 12) in order to determine the unknowns of the problem is performed through an approximation of these variables in total time interval $I_t = [t_0, t_f] = \cup_{n=0}^{Nt}[t_n, t_{n+1} = tn + \Delta t]$. Δt is the increment between two successive time steps. This approximation is done for every integration point related to every finite element following the robust finite element method.

Thus knowing the initial variables at t_n, the discretized problem is solved giving the final solution at the final time t_{n+1}.The discretization leads to the following expressions of the problem variables at $t_{n+1}=t_n+\Delta t$, the end of the step time:

$$\underline{\sigma}_{n+1} = (1 - D_{n+1})\left(\lambda tr\, \underline{\varepsilon}^{e}{}_{n+1}.I + 2\mu\underline{\varepsilon}^{e}{}_{n+1}\right) \quad (13)$$

$$\underline{\varepsilon}^{e}{}_{n+1} = \underline{\varepsilon}^{e}{}_{n} + \Delta\underline{\varepsilon}^{e}{}_{n} \quad (14)$$

$$Y_{n+1} = \frac{1}{2}\underline{\varepsilon}^{e}{}_{n+1} : \underline{\underline{A}} : \underline{\varepsilon}^{e}{}_{n+1} \quad (15)$$

$$f_{n+1} = Y_{n+1} - \frac{1}{2}Y_0 - mD_{n+1}{}^{\frac{1}{s}} = 0 \quad (16)$$

From this last equation the "admissible" value of the damage variable is deduced as: $D_{n+1} = \langle\frac{Y_{n+1}-\frac{1}{2}Y_0}{m}\rangle^{s}$ (17)

In this isotropic damage modeling, some remarks can be made:

- If the scalar variable describing damage D=0, then the material state is described by the classical isotropic elastic model.
- If the fracture condition of the critical value of D=1 is reached. D=0.999 is then assigned to theoretical damage value for numerical consideration and the state of final fracture.

We will call the damage prediction combined with the first method (eq 1) model 1, the one that is coupled with the second method (eq2), model 2. Finally, the damage model associated with the third method (eq 4) will be called model 3.
These three damage models and the cracks propagation technique have been implemented into the FE code Abaqus/Standard via the user subroutine VMAT which uses an explicit integration method to solve the nonlinear problem.

3. Simulations

- Boundary and Loading conditions

In general, the fracture of the vertebra occurs when the bone is subjected to a high compression load. A compressive pressure is applied then to the upper surface and the lower surface is constrained, (Figure4). The computations were carried out using the kill element method. This method simulates the propagation direction by setting the stiffness matrix to zero when the critical damage value (D=0.999) is reached inside an element of the mesh. This leads to the distribution of the stress state in the damage area. The pressure loading the vertebra is calculated from the experimental load obtained throughout the previous testing presented in section 1.

4. Results

As mentioned previously, the purpose of this work is to predict effectively the damage localization as well as the ultimate fracture strength for different specimens tested experimentally and presented in section 1.2. The ultimate strength load value obtained experimentally was applied for the three numerical models presented in section 2.1. The nonlinear analysis showed that the localized damaged zones were found to be different for each model. The results of the fitting of computed and experimental data are described in the next paragraph. The parameters Y_0, m and s used in equation (11) have been chosen for every vertebra to best fit the experimental data.

The predicted load–displacement curves based on the variation of the young's modulus models (model1, model 2, model 3) presented in figure 5 have been obtained for the specimen 2-L2 and specimen 3-L2. The two chosen curves have been selected among the six experimental ones from figure 3. They have the highest and the lowest value of ultimate loads. The figure showed a similarity between the experimentally quasi- brittle failure and the numerical obtained results obtained and the best results are found when the quasi-brittle law is combined with for the Hernandez law (model 3) for the healthy vertebra (specimen 3-L2). It showed also that the predicted crack path with different stages of damage localization for the same vertebra. It is obvious that the two curves fit when damage reaches the value of 0.22 which means that the two curves tend to be similar when the damage starts to grow. The ultimate fracture load under compression (3.8±0.21 KN) that occurs for the critical value D=0.52. Indeed, for compression the critical damage can be reduced to the value D= 0.5 [41]. The strong damage accumulation occurs in inner of the vertebra as mentioned in [11] leading to the

crush of the vertebral body as observed experimentally (Figure1b).The numerical curve obtained by model 2 showed a similarity in the value of the ultimate fracture load (4.79 ± 0.91 KN) but with a permanent shift toward the experimental curve. For the osteoporotic vertebra (specimen 2-L2) the comparison between the numerical result predicted by the model 1 and the experimental data (0.682 ±0.265 KN) shows a good agreement. However, the damage localization in that case is on the top of the vertebra (Figure 5). A better similarity is obtained for the same osteoporotic vertebra from the model 2 with crack localization in the middle of the vertebra as it will be detailed in Figure 6.

Table 3 summarizes the obtained computed ultimate loads for the six vertebrae. The standard deviation SD for the models 1, 2 and 3 were respectively included in the intervals [0.265; 2.14], [0.027; 0.91], and [0.048; 0.446]. Model 3 is then the most accurate one since it gives the lowest difference in comparison with the experimental data.

Figure 6 shows that in case we choose model 1, the damage localization is on the top of the vertebra with low value of critical damage [0.177; 0.392]. When we choose model 2 and 3, a good localization is obtained [0.478; 0.57]; i.e. in the middle of the vertebra (as observed experimentally). The choice of model 1 leads to a localization zones located on the top of vertebrae for all computed cases.

From the latest results, it is concluded that the choice of model 1 (apparent density based Young's modulus model) is more relevant for the osteoporotic vertebra; however it gives a localization on the top of the specimen. Numerical model3 expressing exclusively the dependency of Young's modulus on the tissue morphology bone fracture BV/TV is suitable for healthy vertebra (good crack localization). The choice of model 2 (including the value of E_T and BV/TV) did give the acceptable results for both vertebra cases (osteoporotic or healthy) with good damage localization.

5. Discussion

The aim of this work was to develop a simple quasi-brittle model to describe the process of vertebral fracture and to compare it to the experimental load-displacement curves. Constitutive equations were developed using a CDM model to be the best to fit to the experimental data. The results of the numerical investigation showed the capabilities of the proposed FE element model to describe and predict the localization of vertebra failure based on the choice of the right modulus, parameters of the evolution damage law (Y_o, s, m) which are hard to obtain experimentally. The accuracy of the results is improved by the use of the BM/TV ratio measured for each vertebra. The quasi brittle isotropic models which are so simplistic can then predict plausibly the compression of bones. The results show that the numerical force-displacement curve using the proposed behavior laws are adequate. This is due to the quasi-brittle isotropic models that made plausible prediction about the results related to the experimental force-displacement curve. The obtained results in this work clearly indicate the dependency of Young's modulus model on the vertebra classification. Adjustment of models can be then applied depending on the BMD of every specific studied case.

It has to be noticed that the numerically predicted load-displacement curves was different from the experimental curves when the value of D was very low. This means that the damage models overestimate the damage at the beginning of the load-displacement curves. The presented numerical models based on an isotropic elastic behavior for bone structure give some good quantities and qualitative results. A correlation between micro and macro mechanisms is suitable to better understand the

whole physical process of damage in order to enhance the damage modeling. Other behavior models should be then chosen like the ones proposed in [42] based on crushable foam plasticity models (an approximation of Tsai-Wu yield function). In addition, for vertebrae highly affected by osteoporosis, 3matic presents some limitation on the quality of the bone structure meshing. Besides, it is the continuum level is largely depending on both elements size and orientation and accordingly the mesh size should be accurately determined for each type of material [43, 44, and 45]. Another limitation of this study was the inclusion of only six samples. This was due to the complexity to generate finite elements meshes. Further studies including more appropriate FE meshing algorithm are indeed necessary to treat the mesh dependency problem. However, despite these limitations, the CDM modeling did show some real potential to predict the right localization of fracture for different types of vertebra (healthy or osteoporosis)**.**

6. Conclusion

The purpose of this work was to develop and validate a simple FE model based on continuum damage mechanics in order to simulate the complete force–displacement curve of lumbar vertebra failure. The quasi-brittle law prediction bone failure corroborates the experimental response of vertebral bone failure under a quasi-static compression loading. The obtained results show important similarities for both models (model 2 and 3) for healthy vertebra and the significant differences emerged for model 1. For osteoporotic vertebrae, the model 1 seems to be more appropriate. Despite these differences, the potential of the CDM model combined with the right young modulus law is proved through the computed results. In general, concerning FE simulations, the combination of the parameters like geometry and BV/TV (QCT) and the BMD measurement (DXA) did improve the numerical results.

References

1. Consensus development conference: “diagnosis, prophylaxis, and treatment of osteoporosis”. Am J Med. 1993 June;94(6):646–50.
2. Kanis JA. , “Diagnosis of osteoporosis and assessment of fracture risk”. Lancet LondEngl. 2002 Jun 1;359(9321):1929–36.
3. Lips P, Van Schoor N.M. “Quality of life in patients with osteoporosis”. OsteoporosisInt J Establ Result Coop Eur Found Osteoporosis Natl Osteoporosis Found USA. 2005 May;16(5):447–55.
4. Kendler D.L, Bauer D.C, Davison K.S, Dian L, Hanley D.A, Harris S.T,”Vertebral Fractures: Clinical Importance and Management”. Am J Med. 2016 Feb;129(2):221.e1-10.
5. Marshall D, Johnell O, Wedel H,” Meta-analysis of how well measures of bone mineral density predict occurrence of osteoporotic fractures”. BMJ. 1996 May 18;312(7041):1254–9.
6. Schuit SCE, Van der Klift M, Weel AE a. M, de Laet CEDH, Burger H, Seeman E, & al.,“Fracture incidence and association with bone mineral density in elderly men and women: the Rotterdam Study”. Bone. (2004 Jan);34(1):195–202.
7. Mccreadie BR, Goldstein SA.,“Biomechanics of Fracture: “Is Bone Mineral Density Sufficient to Assess Risk?”, J Bone Miner Res. 2000 Dec 1;15(12):2305–8.
8. Doblare M., Garcia J.M.,“Anisotropic bone remodeling model based on a continuum damage-repair theory”, Journal of Biomechanics 35 (2002)1–17.
9. Doblare M, , Garcıa-AznarJ.M. ,“On Numerical Modeling of Growth, Differentiation and Damage in Structural Living Tissues”, Arch. Computer . MethodEngineering. (2006), Vol. 13, 4, 471-513.
10. Ramtani.S,. GarciaJ.M, DoblareM, “Computer simulation of an adaptive damage-bone remodeling law applied to three unit-bone bars structure”. 2004. Computers in Biology and Medicine 34:259–273
11. Garcia D, Zysset Ph. K, Charlebois M, A Curnier A, “ A three-dimensional elastic plastic damage constitutive law for bone tissue”, Biomechanical Model Mechanobiol (2009),8:149-165.
12. Hambli R,“A quasi-brittle continuum damage finite element model of the human proximal femur based on element deletion”, Med Biol Eng Comput 51, 1-2 (2013) 219-3.
13. Hambli R, Bettamer A, AllaouiS, “Finite element prediction of proximal femur fracture pattern based on orthotropic behavior law coupled to quasi-brittle damage , Medical Engineering & Physics 34 (2012) 202– 210.
14. Schileoa E, Taddeia F, Cristofolinia L,Viceconti M, ”Subject-specific finite element models implementing a maximum principal strain criterion are able to estimate failure risk and fracture location on human femurs tested in vitro”, Journal of Biomechanics 41 (2008) 356–367
15. Zysse Ph.K, Curier A, “A 3D Model for Trabecular bone based on fabric tensors”,Journal of Biomechanics 29 (1996) 1549–1558).

16. Mengoni M, PonthotJ.P., “A generic anisotropic continuum damage model integration scheme adaptable to both ductile damage and biological damage-like situations”. International Journal of Plasticity (2015)66: 46–70.
17. Ulrich D, B, LaibA, P Ŕuegsegger,”The ability of three-dimensional structural indices to reflect mechanical aspects of trabecular bone”, BONE, (1999), Volume 25, Issue 1, Pages 55–60
18. KowalczykP,“Elastic properties of cancellous bone derived from finite element models of parameterized microstructure cells” ,Journal of Biomechanics 36 (2003) 961–972
19. Elise F. Morgan E.F, Bayraktar H.H,Keaveny T.M, “Trabecular bone modulus–density relationships depend on anatomic site ”, ,Journal of Biomechanics 36 (2003) 897–904
20. Gibson, L.J., “The Mechanical behavior of calcellous bone”, J. Biomechanics Vol. 18. No. 5. pp. 317-328. 198
21. Cowin S.C., Van Buskirk W.C., “Thermodynamic restriction of the elastic constants of bone”, J. Biomechanics (1986), Vol. 19. Ho I. pp. 85-87.
22. Yang,G**,** Kabel J, Van Rietbergen, B., Odgaard, A., Huiskes, R., and Cowin, S.C., “The Anisotropic Hooke’s Law for Cancellous Bone and Wood”.Journal of Elasticity**53**(1999)**:** 125–146,.
23. Hernandez ,C. J., Beaupré, G.S., T. S. Keller, T.S., and Carter, D.R. ,“The Influence of Bone Volume Fraction and Ash Fraction on Bone Strength and Modulus ”, Bone Vol. 29, No. 1, July 2001:74–78
24. Jacobs, C.R.,“Numerical Simulation of Bone Adaptation to Mechanical Loading”. Ph.D. Thesis, Department of Mechanical Engineering – Stanford University. 1994.
25. Keyak J.H., Meagher J.M., Skinner H.B., Mote Jr., C.D, “Automated three-dimensional finite element modeling of bone: A new method”, J. Biomedical Engineering, vol 12(1990) 389.397.
26. Helgason B, Perilli E, Schileo E, Taddei F, Brynjolfsson S, Viceconti M, “Mathematical relationships between bone density and mechanical properties : A literature review”, Clinical Biomechanics, vol 23(2008). p 135-146.
27. Madi.K, Forest.S, Boussuge.M, Gailliègue.S, Lataste.E, Buffière J-Y, Bernard.D, Jeulin.D, “ Finite element simulations of the deformation of fused-cast refractories based on X-ray computed tomography”. Computational Materials Science, vol 39 (2007), p 224-229
28. Tawara D, Sakamoto J, Murakami H, Kawahara N, Oda J, Tomita K, “ Mechanical evaluation by patient-specific finite element analyses demonstrates therapeutic effects for osteoporotic vertebrae”, The Mechanical behavior of biomedical materials,vol 3 (2010), p 31-40
29. Jovanovic J.D, JovanovicM.Lj , “Finite element modeling of the vertebra with geometry and material properties retrieved from CT-Scan Data. Mechanical Engineering , vol 8 (2010) , p 19-26
30. Gislason M.K, Ingvarsson P,Gargiulo P,Yngvason S, Guomundsdottir V, Knutsdottir S, Helgason P, “Finite element modeling of the femur bone of a

subject suffering from motor neuron lesion subjected to electrical stimulation", Eur J Trans Myol-Basic ApplMyol, (2014), 24 (3) 187-193
31. Magerl F, Aebi M, GertzbeinS.D, Harms J, NazarianS.," A comprehensive classification of thoracic and lumbar injuries". EuroSpine J. (1994); 3: 184-201
32. Louis Ch, Nazarian S, Louis R," Comment nous traitons les fractures récentes du rachis thoraco-lombaire", dans la catégorietechnique,Hôpital de la conception – Marseille, Maitrise Orthopédique,,N°58 – Novembre 1996.
33. Clouthier A.L, Hosseini H.S, Maquer G, Zysset Ph.K "Finite element analysis predicts experimental failure patterns in vertebral bodies loaded viaintervertebral discs up to large deformation", Medical Engineering and Physics 37 (2015) 599–604
34. Chaboche J.L, "Continuum Damage Mechanics ", Part I and II, Journal of Applied Mechanics, (1988) ,vol 55, pp 59-79,
35. Germain P," Mécanique des Milieux" continus, Paris: Masson, 1973.
36. Kracinovic D, " Damage Mechanics", Mechanics of Material (1989) 8: 127,
37. Saanouni K, Forster Ch, Ben Hatira F, " On the Anelastic flow damage", International Journal of Damage Mechanics (1996), pp 140-169.
38. Lemaitre J, " Formulation Unifiée de lois d'évolution d'endommagement", C.R Acad, Sci, Paris, 305, Serie II, pp 1125-1130.
39. Kachanov L.M, "Introduction to Continuum Damage Mechanics", Netherlands; Martinus Nijhokk Publishers, 1986.
40. Marigo J.J, "Formulation of a damage law for an elastic material". Comptes Rendus, Serie II-Mécanique, Physique, Chimie, Sciences de la Terre.(1981) , 1390-1312.
41. Hambli R., "Multiscale prediction of crack density and crack length accumulation in trabecular bone based on neural networks and finite element simulation", International Journal for Numerical Methods in Biomedical Engineering,2011, (27):4,461–475.
42. Kinzi M, Wolfman U, PahrD.H., "Identification of a crushable foam material model and application to strength and damage predication of human femur and vertebral body", Journal of the mechanical behavior of biomedical material 26 (2013), 136-147.
43. Hoffler, C.E., McCreadie, B.R., Smith, E.A., and Goldstein, S.A. Hierarchical testing of trabecular and cortical bone. In Mechanical Testing of Bone and the Bone-Implant Interface, Y.H. An and R.A. Draughn, (Eds.), CRC Press, Boca Raton, FL, 1999;
44. Buechner, P.M. and Lakes, R.S. "Size effects in the elasticity and viscoelasticity of bone3. Biomechanics and Modeling in Mechanobiology",(2003). 1(4): 295-301.
45. Bredbenner T.L, Nicoletta D.P, Davy D. T ," Modeling damage in human vertebral trabecular bone under experimental loading. Experimental Mechanics", Conference paper, January 2006.
46. Mirzaei M, Zeinali A , Razmjoo A, Nazemi M, "On prediction of the strength levels and failure patterns of human vertebrae using quantitative computed

tomography (QCT)-based finite element method", Journal of Biomechanics 42 (2009). 1584–1591
47. Linde, F., Hvid, I., Madsen, F.,. "The effect of specimen geometry on the mechanical behavior of trabecular bone specimens", Journal of Biomechanics 25(1992) .359–368.
48. Carter, D.R., Hayes, W.C., "The compressive behavior of bone as a two-phase porous structure. Journal of bone and joint surgery. American volume (1977.954–962.
49. Snyder, S.M., Schneider, E., "Estimation of mechanical properties of cortical bone by computed tomography" , Journal of Orthopaedic Research 9 (1971), 422–431.
50. Kaneko, T.S., Bell, J.S., Pejcic, M.R., Tehranzadeh, J., Keyak, J.H.," Mechanical properties, density and quantitative CT scan data of trabecular bone with and without metastases". Journal of Biomechanics 37 (2004). 523–530.

Table 1. : Failure values for the six lumbar vertebrae.

Specimen	vertebra	BMD (g/cm2)	Load (KN)	Displacement (mm)
1	L2(healthy)	1.016	1.615	7
2	L2(Osteoporotic)	0.616	1.057	9.87
3	L2(healthy)	0.884	3.501	4.6
3	L3(healthy)	0.938	3.074	9.14
3	L4(healthy)	0.881	2.839	5.77
4	L2 (Osteoporotic)	0.819	2.437	8.4
SD		0.136	0.924	2.037

Table 2.1 : Material properties for bone used for the simulation (specimen 2–L2)

GR : E = 3500 $\rho^{2.2}$					
	Density (g/cm3)		Young ’s Modulus (MPa)	Poisson ratio	
Cortical bone	0.64-2.09		1330-17859	0.3	
Concellous bone	0.04-0.41		4-517	0.3	
Yang´s Law : E = 1240 * ET * (BV/TV) $^{1.80}$					
	Density (g/cm^3)	BV/TV	Young ‘s Modulus (MPa)	Poisson ratio	E_T
Vertebra	0.03-1.74	0.3	993.89	0.3	7
Hernandez´s Law : E = 84370*(BV/TV) $^{2.58}$					
	Density (g/cm^3)	BV/TV	Young ‘s Modulus (MPa)	Poisson ratio	
Vertebra	0.03-1.74	0.3	3777.12	0.3	

Table 2.2 : Material properties for bone used for the simulation (specimen 3–L2)

GR : $E = 3500\ \rho^{2.2}$					
	Density (g/cm^3)		Young's Modulus (MPa)	Poisson ratio	
Cortical bone	0.619-1.89		1219-14299	0.3	
Cancellous bone	0.05-0.414		6-505	0.3	
Yang´s Law : $E = 1240 * ET * (BV/TV)^{1.80}$					
	Density (g/cm^3)	BV/TV	Young's Modulus (MPa)	Poisson ratio	E_T
Vertebra	0.05-1.89	0.3	5537.38	0.3	39
Hernandez´s Law : $E = 84370*(BV/TV)^{2.58}$					
	Density (g/cm^3)	BV/TV	Young Modulus (MPa)	Poisson ratio	
Vertebra	0.05-1.89	0.3	3777.12	0.3	
Resin	1.2		4220	0.4	

Table 3: Ultimate computed load (SD) for the six specimens

	Specimen 1-L2	Specimen 2-L2	Specimen 3-L2	Specimen 3-L3	Specimen 3-L4	Specimen 4-L2
Numerical (Model 1)	1.037(0.408)	0.682 (0.265)	0.467(2.145)	1.131(1.373)	1.898(0.665)	0.759(1.17)
Numerical (Model 2)	2.074 (0.324)	0.977(0.056)	4.796(0.915)	3.035(0.027)	3.576(0.5211)	1.478(0.661)
Numerical (Model 3)	1.712 (0.068)	1.274 (0.153)	3.805(0.215)	3.142(0.048)	1.782(0.446)	1.782(0.446)

Figure 1 **:** Flow chart showing the protocol established to create FE models from CT data using material properties.

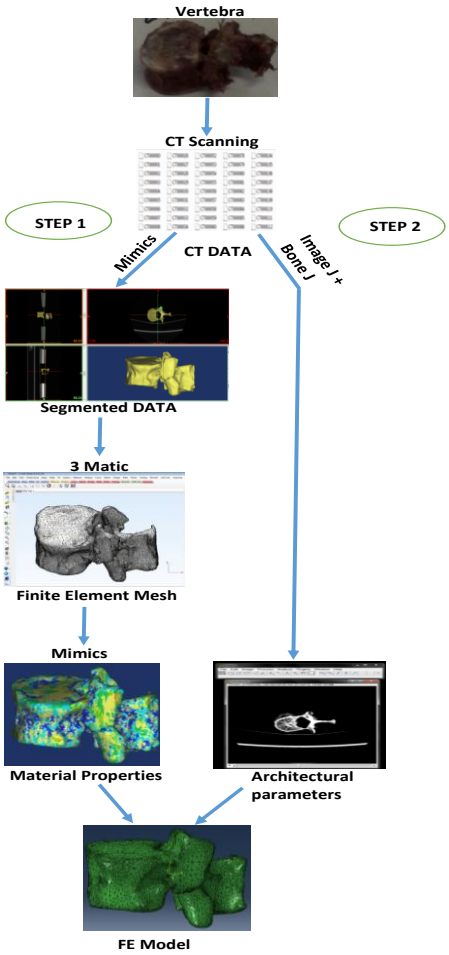

Figure 2 a **:** Lumbar vertebra before failure. The resin is placed at the top and the bottom of the vertebral body.

Figure 2b: Lumbar vertebra after failure. Localization of the fracture at the middle of the vertebral body.

Figure 3 : Experimental load vs. displacement for the six specimens with the indication of each vertebra tangent modulus E_T (MPa) and the value of every specimen BMD.

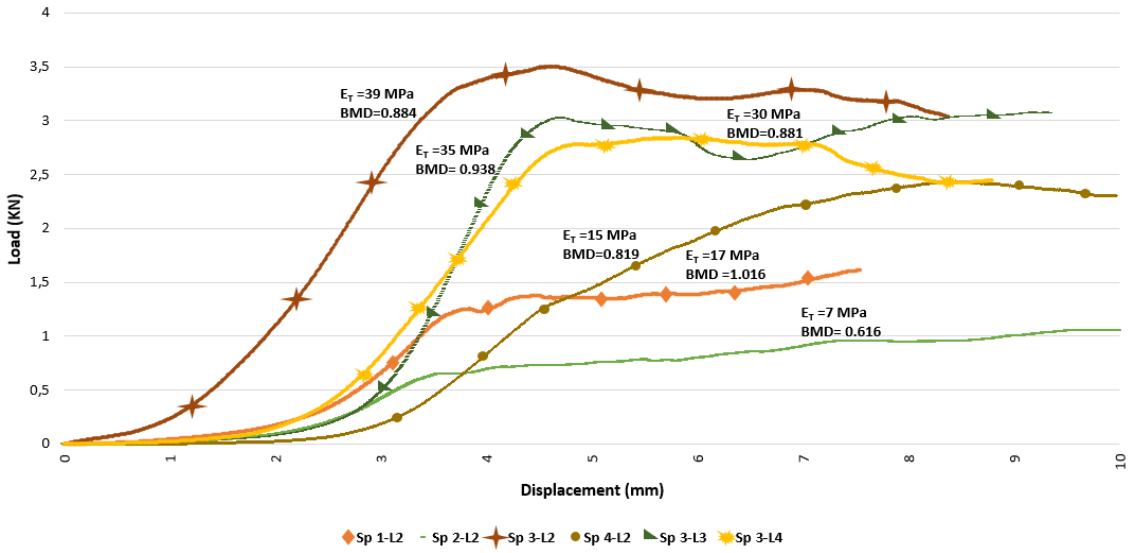

Figure 4: Vertebra Load and boundary conditions (Meshing of the specimen 3-L2 using 81473 linear tetrahedral elements)

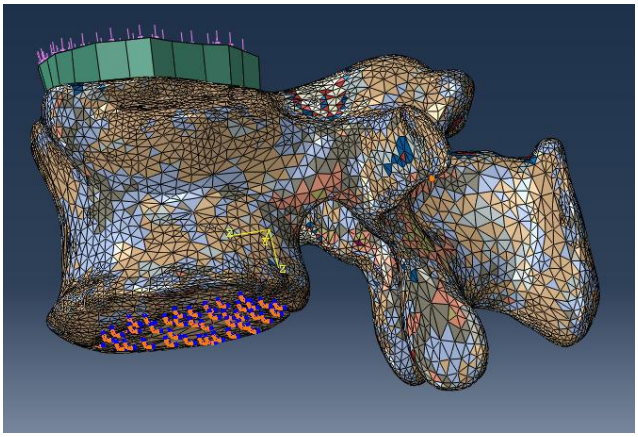

Figure 5: Experimental and computed load vs displacement curves during the compression of two vertebrae with the two different numerical models. Damage distribution at different displacement values as predicted with model 2 for the specimen 2-L2 and with model 3for specimen 3-L2.

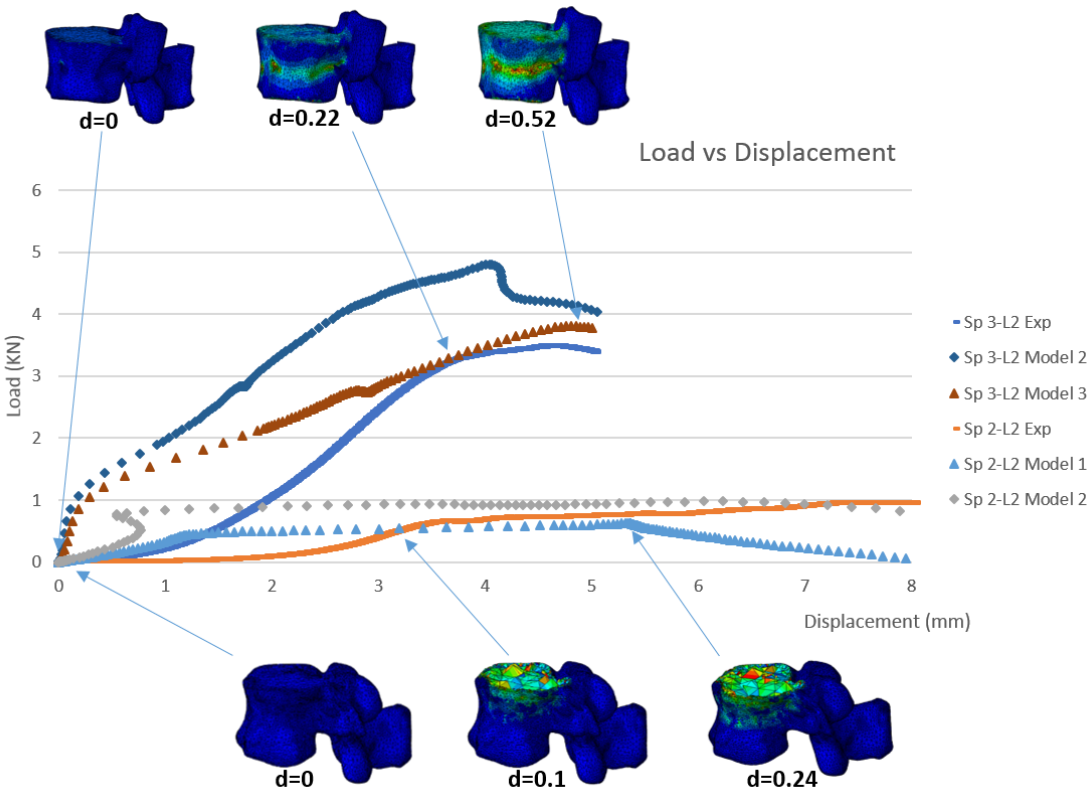

Figure 6: CT- Scan and F-E results for the six specimens: Damage localization zones when the ultimate experimental load is reached for the three models.